

**Reconsidering Emissions of Ammonia from Chemical Fertilizer Usage in
Midwest USA**

**Srinidhi Balasubramanian¹, Sotiria Koloutsou-Vakakis^{1,*}, D. Michael McFarland² and
Mark J. Rood¹**

¹ Department of Civil and Environmental Engineering, University of Illinois at Urbana-
Champaign, Urbana, Illinois, USA

² Department of Aerospace Engineering, University of Illinois at Urbana-Champaign, Urbana,
Illinois, USA

* Correspondence to: S. Koloutsou-Vakakis, Department of Civil and Environmental
Engineering, University of Illinois at Urbana-Champaign, Urbana, Illinois, 61801, USA
(sotiriak@illinois.edu)

Key Points

- Method developed to model NH₃ emissions from chemical fertilizer usage
- Spatial allocation of emissions based on crop location and nitrogen management
- Temporal emission variations based on a biogeochemical model

Abstract

We present alternative methods for estimating spatial surrogates and temporal factors for ammonia (NH₃) emissions from chemical fertilizer usage (CFU), in USA, at spatial and temporal scales used to simulate regional air quality and deposition of reactive nitrogen to ecosystems. The newly developed Improved Spatial Surrogate (ISS) method incorporates year specific fertilizer sales data, high resolution and year specific crop maps, and local crop nitrogen demands to allocate NH₃ emissions at 4 km x 4 km grid cells. Results are compared with the commonly used gridded emission estimates by the Sparse Matrix Operator Kernel Emissions (SMOKE) preprocessor. NH₃ emissions over Central Illinois in USA, estimated at the 4 km x 4 km grid level in SMOKE and ISS methods exhibit differences between -10% and 120%, with 58% of the grid cells exhibiting more than $\pm 10\%$ difference. Application of the ISS method for a larger domain over the Midwest USA, at 4 km x 4 km, reflected similar differences. We also employed the DeNitrification DeComposition (DNDC) model to develop daily temporal factors of NH₃ emissions from CFU using multi-site and multi-year analyses. Ratio of temporal factors estimated by SMOKE and DNDC methods is 0.54 ± 2.35 , with DNDC identifying daily emission peaks 2.5-8 times greater than SMOKE. Identified emission peaks will be useful for future air quality modeling efforts to understand particulate matter episodes, as well as, trends in

38 regional particulate matter formation and nitrogen deposition for Midwest USA, using the
39 proposed NH₃ emissions inventory.

40

41 **Keywords**

42 Ammonia emissions, chemical fertilizer usage, DNDC, SMOKE, temporal factors, spatial
43 surrogates

44

1. Introduction

Increasing demand for food and biofuel production for a growing population has resulted in the introduction of fixed reactive nitrogen (Nr) in the environment, in quantities surpassing those fixed by natural pathways [Galloway *et al.*, 2003; Erisman *et al.*, 2007]. One of the adverse impacts of chemical fertilizer usage (CFU) is the emission of NH₃ to the atmosphere. NH₃ is a precursor to PM₁₀ and PM_{2.5} (particulate matter with diameters $\leq 10 \mu\text{m}$ and $\leq 2.5 \mu\text{m}$, respectively) that are regulated for their adverse impacts on human health and visibility [WHO, 2005; EEA, 2012; U.S. EPA, 2012]. Atmospheric transport and subsequent deposition of NH₃, and its secondary products from chemical reactions in the atmosphere, also result in surface water eutrophication, soil acidification and acceleration of biodiversity loss [Pardo *et al.*, 2011; Erisman *et al.*, 2013]. In USA, NH₃ is predominantly emitted from agricultural sources like concentrated animal feeding operations (55%) and CFU (26%) [U.S. EPA, 2013]. In the Midwest USA, contributions from CFU to NH₃ emissions (54%) are much higher compared to USA (26%) because of fertilizer-intensive crop management [U.S. EPA, 2013]. Emissions from such intensively fertilized regions (called hotspots henceforth, for brevity) are important for regional air quality. As an example, a recent study found enhancement of PM_{2.5} concentrations in USA Great Lakes region that corresponded almost entirely to an increase in ammonium in the particles [Stanier *et al.*, 2012].

Reductions in NH₃ emissions from agricultural sources has been proposed as a cost-effective way to attain National Ambient Air Quality Standards for PM_{2.5} in the future [Pinder *et al.*, 2007]. This is important because while emission reductions of PM precursors of sulfur and nitrogen oxides have been achieved due to implementation of control technologies, future reductions are expected to be costly [U.S. EPA, 2003]. These emission reductions would also

result in an increase of gaseous atmospheric NH₃ concentrations, alter PM_{2.5} composition to less acidic particles [Pinder *et al.*, 2008] and shift nitrogen deposition closer to emission sources [Saylor *et al.*, 2014]. Previous studies have documented the need for spatially and temporally accurate NH₃ emission inventories to improve predictions of historical and future PM trends [Wu *et al.*, 2008; Henze *et al.*, 2009]. Of particular interest are NH₃ emissions from CFU that are highly uncertain [Appel *et al.*, 2011; U.S. EPA, 2011], due to the large number of variables that control NH₃ volatilization, such as fertilizer type, soil properties, weather conditions and canopy characteristics [Sharpe and Harper, 1995; Bouwman *et al.*, 2002; Sommer *et al.*, 2004]. A small number of measurement studies in USA have examined correlations between NH₃ volatilization and its controlling factors. Examples include short-term measurements in North Carolina over a corn canopy [Bash *et al.*, 2010; Walker *et al.*, 2013], unfertilized soybean canopy [Walker *et al.*, 2006; Myles *et al.*, 2011], short grass [Phillips *et al.*, 2004] and multiple crop canopies in California [Potter *et al.*, 2001].

Current estimates of NH₃ emissions from CFU in the National Emissions Inventory (NEI) are based on a top-down approach [Goebes *et al.*, 2003]. Emissions are estimated by combining annual fertilizer sales data reported at the county level [AAPFCO and The Fertilizer Institute, 2014] with fertilizer-specific emission factors adopted from the European Environment Agency (EEA) [Asman, 1992]. While availability of farm-specific CFU practices can support an improved emissions inventory [Bouwman *et al.*, 2002], such detail is unavailable for USA. Similarly, in view of the sparse measurements of NH₃ emissions, EEA emission factors provide a proxy to estimate the top down NH₃ emissions for the environmental conditions and crop management practices present in USA [Aneja *et al.*, 2008]. NEI emissions are then processed through the Sparse Matrix Operator Kernel Emissions (SMOKE) model [CMAS, 2013] to

provide inputs at spatial and temporal resolutions needed for chemical transport models (CTMs). Allocation of emissions within SMOKE introduces additional uncertainties. SMOKE is used to bridge the spatial resolution of emissions from the county level to the CTM grid using spatial surrogates [U.S. EPA, 2005]. NH₃ emissions are distributed in proportion to the area of agricultural land in the grid cell as indicated by the National Land Cover Database (NLCD) [Vogelmann *et al.*, 2001]. This approach does not consider differences in emissions arising from CFU, which depends on crop-specific nitrogen demand and crop rotation. Temporal resolution within SMOKE is converted from the annual scale reported by NEI to the hourly scale required by CTMs using temporal factors that are defined as the percentage of emissions arising in each hour of the year [U.S. EPA, 2002]. These temporal factors are based on seasonal data of nitrogen application [USDA, 1997] and are estimated in proportion to the amount of nitrogen applied in each crop period. A more detailed description is provided in Section 2.3.1.

Studies have attempted to validate spatial and temporal distributions of NH₃ emissions through CTM predictions of ambient NH₃, NH₄⁺ and PM concentrations [Wu *et al.*, 2008; Appel *et al.*, 2011], inverse modeling techniques [Gilliland *et al.*, 2006; Paulot *et al.*, 2014] and satellite measurements of NH₃ concentrations [Pinder *et al.*, 2011; Zhu *et al.*, 2013]. These studies attribute underestimations in modeled NH₄⁺ wet deposition in winter and spring and overestimations in summer and fall [Appel *et al.*, 2011] and errors in modeled ambient ammonium nitrate concentrations [Heald *et al.*, 2012] to uncertainties in magnitude and seasonality in NH₃ emissions from CFU, at regional scales.

Studies have attempted to incorporate crop management data and environmental variables to develop temporal factors to replace the existing static NH₃ emission profiles for CFU that are constant across years [Pouliot *et al.*, 2012]. These efforts include development of process based

models like VOLT' AIR [Genermont and Cellier, 1997] that estimate emissions based on the physical and chemical equilibria between different nitrogen species in the soil, soil aqueous phase and the atmosphere. Dynamical models have also been developed to estimate temporal variations in NH₃ emissions at the hourly scale based on diurnal variations in temperature and wind speed [Gyldenkerne et al., 2005; Skjøth et al., 2011]. The Magnitude and Seasonality of Agricultural Emissions model (MASAGE) has adopted similar semi-empirical relations to estimate emissions across different climatic regions at spatial resolution of 0.5° x 0.5°, reported at a resolution of three hours [Paulot et al., 2014]. While these efforts have collectively aimed at improving seasonality of NH₃ emissions from CFU, availability of farm-specific CFU data is an outstanding challenge.

In this paper, we present an alternative approach that is intended to be readily integrated with the existing approach of using NEI and SMOKE to prepare inputs for CTMs. Compilations of emission inventories for area sources are data and resource-intensive. In the following sections, we present a new method for developing NH₃ emissions from CFU by incorporating (a) available grid cell-level information to improve spatial resolution and (b) estimates from a biogeochemical model to obtain temporal variability profiles. These results are presented and compared with the approach of using NEI-based, SMOKE-gridded and temporally allocated emissions. Our approach is scalable to different spatial resolutions and different spatial domains.

2.0 Methods

2.1 Study domain

Illinois was the second largest consumer of chemical-based nitrogen fertilizers (8.3%) in USA in 2011 [NASS, 2014b]. Due to challenges with identification of available data sources, and

requirements for computational resources, a test domain was first chosen in central Illinois (Figure 1a) for method development, which was then expanded to a larger domain over Midwest USA (Figure 1b) that includes the states of Illinois, Indiana, and Missouri and parts of Iowa, Kansas, Kentucky, Michigan, Nebraska, Oklahoma, Ohio and Tennessee. A measurement site for measuring NH₃ emissions fluxes from a corn canopy [Myles *et al.*, 2014; Nelson *et al.*, 2014] is also located centrally in this domain to facilitate future comparisons with this modeling study. The Improved Spatial Surrogate (ISS) method has been developed in this study to allocate emissions down to a 4 km x 4 km grid, based on differential crop nitrogen demands. Emission inputs to CTMs like Community Multiscale Air Quality (CMAQ) model and Comprehensive Air Quality Model with Extensions (CAMx) have typically been run at resolutions of 12 km x 12 km or 36 km x 36 km. Temporal trends in NH₃ emissions and variations were modeled at the daily scale by using the biogeochemical model DeNitrification DeComposition (DNDC) [Li *et al.*, 1992]. ArcGIS 10.2 [ESRI, 2013] and MS Access [Microsoft, 2013] were used to manage, analyze and visualize spatial data.

2.2 Identifying Spatial Variations in NH₃ Emissions at High Spatial Resolutions

In SMOKE, spatial allocation of NH₃ emissions from CFU from county to CTM grid resolution is based on NLCD for the year 1992 [Vogelmann *et al.*, 2001]. Spatial Surrogate Ratios (SSRs) are used to allocate emissions from the county to CTM grid resolution. SSRs are calculated as the ratio of agricultural area in each grid to the total agricultural area in the county [U.S. EPA, 2005]. In the newly developed ISS method, we use the high spatial resolution Cropland Data Layer (CDL) maps [NASS, 2014c] as the spatial surrogate of choice. These maps provide the advantage of identifying specific crops in the domain of interest in a given study

year, compared to the five general categories in NLCD, for the year 1992. CDL maps provide information on location and extent of 108 crops in year 2002 and 131 crop types in year 2011 within the contiguous USA. Additionally, we developed a new SSR formulation, to account for the differential nature of CFU based on crop nitrogen demands that are reported for different states in USA (Table 1). Crop nitrogen demand is defined as the average nitrogen applied per hectare for the year closest to the year considered in the analysis [NASS, 2014b]. The ISS method implements SSRs that are estimated by normalizing crop area in each grid with crop-specific nitrogen demand [NASS, 2003]. To resolve the mismatch in spatial resolution between the 4 km x 4 km ISS domain and 30 m x 30 m CDL grid sizes, we added the 30 m x 30 m crop areas that were included in each respective 4 km x 4 km grid. NH₃ emissions at 4 km x 4 km grid level for the domains described above were estimated from county-level fertilizer sales data and NH₃ emission factors for CFU from Goebes et al. [2003] and downscaled from county scale to the 4 km x 4 km using the SSRs developed for the ISS method.

Only 17 of the 108 crops were present in the Central Illinois domain and considered for estimating emissions, for the year 2002. Of these 17 crops, Illinois specific nitrogen demands were available for 15 crops [NASS, 2014b]. Missing nitrogen demands for oats and barley were obtained from data for the state of Wisconsin [NASS, 2014b]. The approach proved to be robust for application to bigger domains, with additional effort to identify state and crop-specific data and manage differences in data availability from state to state. For example, fertilizer sales data are available only at the state level for 18 states in USA [AAPFCO and The Fertilizer Institute, 2014]. Hence, grid level emissions for these 18 states required a modification in the definition of SSRs. The SSRs were recalculated by considering the crop extent across the entire state instead of at the county level. Surplus sales data within each state were allocated to those counties with

missing sales data in proportion to the area of available cropland. Crop nitrogen demand is defined as the average nitrogen applied per hectare for the year closest to the year considered in the analysis, for each state in the contiguous USA [NASS, 2014b]. Where missing, crop nitrogen demands were gap filled with data obtained either from (a) a neighboring state; (b) a state at a similar latitude or (c) the closest state with available data, in this order. The location of the grid and identification of the crops for the calculation of SSRs, as related to the county and state, were identified within GIS shapefiles with county boundaries [U.S. Census Bureau, 2011]. A unique identification code comprising the crop IDs from CDL and state ID was generated to ensure that the Access database correctly retrieved crop nitrogen demands specific to each state.

2.3 Identifying Temporal Variations in NH₃ Emissions from Chemical Fertilizer Usage on a Daily Scale

2.3.1 Existing Approach in SMOKE to Estimate Temporal Factors

Temporal factors are defined as the percentage of total annual NH₃ emissions emitted hourly for the year under consideration. Temporal factors in SMOKE [U.S. EPA, 2002; Goebes *et al.*, 2003] are first estimated seasonally using nitrogen management data for average nitrogen demand of the crop in the state and the percentage area of crop receiving nitrogen during different crop periods [USDA, 1997]. Crop periods are classified as “at planting”, “after planting”, “fall before planting” and “spring before planting”. Dates specific to these crop periods are categorized using crop planting and harvesting dates [NASS, 2010]. Historic dates of planting and harvesting dates and timing of nitrogen application are available for different regions of USA for major crop types [USDA, 1997; NASS, 2010]. Monthly temporal factors are then estimated from the averaged seasonal temporal factors based on the crop periods considered

for each crop type. Finally, temporal factors are determined at the hourly scale by distributing the monthly emissions equally to each Julian day and then equally to 24 hours, thereby resulting in time-averaged emission estimates.

2.3.2 Proposed Approach in this Study to Estimate Temporal Factors using DNDC

2.3.2.1 Implementing the DNDC Model to Model Temporal Variations in NH₃ Emissions

As previously mentioned, we employed the DNDC model version 95 [Li *et al.*, 1992] to obtain temporal variation of NH₃ emissions at the daily scale. DNDC is widely employed to simulate magnitude and timing of trace gas emissions at the daily or annual scale from managed and natural ecosystems. DNDC has been used to evaluate the impact of crop-rotation and tillage practices on crop yields [Farahbakhshazad *et al.*, 2008], emissions of nitrous oxide [Xu-Ri *et al.*, 2003; Gopalakrishnan *et al.*, 2012], and nitrate leaching into water bodies [Tonitto *et al.*, 2007; David *et al.*, 2009]. DNDC is driven by ecological parameters that describe climate, plant growth and human activities. These ecological drivers modify the soil climate (e.g., soil temperature, moisture, pH, redox potential, and substrate concentration), which then drives the activity of nitrifiers and denitrifiers in the soil [Li, 2000; Xu-Ri *et al.*, 2003]. NH₃ emissions are estimated in the nitrification process that is simulated within the decomposition sub-model.

Crop management practices inputs in the form of CFU dates, crop rotation and nitrogen loading from different fertilizer types are required for DNDC. These data are generally not available at the individual farm level, due to confidentiality considerations. Hence, we developed an approach to estimate site level inputs for timing and amount of different fertilizer usage alongside inputs of crop, soil and weather as outlined in Figure 2 and explained in Section 2.3.2.2. An initial application of this method was demonstrated for the year 2002

[Balasubramanian *et al.*, 2014]. 13 sites were then chosen within the test domain of Central Illinois and modeling runs were conducted over a ten year span of 2002-2011. Study sites correspond to the 4 km x 4 km grids that are co-located with the 13 meteorological stations shown in Figure 1a [Illinois State Water Survey, 2014]. Our goal is to conduct a multi-site and multi-year analysis using these 13 sites to obtain temporal trends in NH₃ emissions applicable to CFU practices typical to Midwest USA.

2.3.2.2 Development of Site-Level Inputs to Initialize DNDC

Estimating Fertilizer Specific Nitrogen-Loading and CFU Dates for Central Illinois

Assumptions were made based on existing agricultural data to develop site level inputs of timing and amount of fertilizer loading. Loading of fertilizer at 4 km x 4 km was estimated by combining the ISS method and county-level fertilizer sales. Contributions from anhydrous ammonia, urea, nitrogen solutions (mix of ammonium nitrate and urea), ammonium nitrate, ammonium sulfate and ammonium phosphates are considered and the chemical form and depth of application was derived from the Illinois Agronomy Handbook [Fernández *et al.*, 2012]. Historic planting and harvesting dates [NASS, 2010] were adopted to identify CFU dates as input to DNDC. These dates describe the range of active planting and harvesting dates for each crop as reported by farmers in Illinois over 20 years. Four planting and two harvesting dates were chosen from the crop schedule data at equal intervals within the crop season in Illinois [NASS, 2010], for each year. This approach resulted in eight combinations of planting and harvesting dates for each crop as inputs to DNDC. An example in estimating timing and amount of CFU to corn is illustrated in Table 2. Trends in timing and loading of nitrogen for corn and soybeans were corroborated by personal communication with Gary Letterly (August 2013) and Emerson

Nafziger (September 2013), both associated with the University of Illinois Extension Program. To summarize, eight days of possible fertilizer input for each crop type was considered. Multi-site, multi-crop and multi-year analysis included inputs for 13 sites, three major crops (corn, soybeans and winter wheat) and 10 years resulting in a total of 1320 modeling runs.

Mapping Weather and Soil Inputs for DNDC

Daily maximum and minimum temperature, precipitation, wind speed, solar radiation and relative humidity were obtained for each of the meteorological stations operated by the Water and Atmospheric Resources Monitoring Program (Figure 1a) [Illinois State Water Survey, 2014]. Nitrogen concentration in precipitation was obtained from the National Trends Network that monitors deposition of inorganic nitrogen as ammonium from the atmosphere [NADP, 2014]. Soil pH, bulk density, organic carbon and clay content for the surface and depths of 5 cm and 10 cm were obtained from the Web Soil Survey [NRCS, 2013] and held constant inter-annually. Conventional tillage practice was assumed and crop residue cover was obtained from the Illinois Agronomy Handbook [Simmons and Nafziger, 2012].

3.0 Results and Discussion

3.1 Distribution of Agricultural Land Receiving Fertilizers

Figures 3a and 3b identify the distributions of agricultural land area receiving CFU accounted by the spatial surrogates within SMOKE and ISS methods respectively, for Central Illinois for the year 2002. Such spatial representation enables inclusion of crop-specific nitrogen demands for SSR calculations in the ISS method. Based on NLCD maps used in SMOKE, agricultural land receiving fertilizers covered 76,446 km² accounting for 73% of the study

domain. Similar analysis with the new surrogate of CDL in our ISS method identified an area of 36,387 km², only 48% of the agricultural area receiving fertilizers originally accounted within SMOKE (Figure 3b). This difference results from ISS method including only the cropland area receiving CFU, while excluding land categories such as pastures, fallow land and crops with zero nitrogen loading in our analysis. SSRs for SMOKE and ISS methods as calculated from Table 1 are shown in Figures 3c and 3d respectively. A visual comparison highlights additional heterogeneity in SSR determined by ISS method as compared to SMOKE. 50% of all grid cells used in the ISS method indicate differences greater than $\pm 20\%$ when compared to SSRs calculated by SMOKE. These new SSRs can be integrated within the SMOKE model to provide emission inputs to CTMs.

3.2 NH₃ Emissions from CFU at 4 km x 4 km Spatial Resolution

3.2.1 Demonstration of ISS Method for Test Domain over Central Illinois for Year 2002

NH₃ emissions from CFU for SMOKE and by ISS methods at 4 km x 4 km are shown in Figures 4a and 4b, respectively. Total emissions represented in the whole study domain in these two figures are the same as both methods are constrained by the same fertilizer sales data. The percent difference in emissions between SMOKE and ISS methods at grid level is shown in Figure 4c. The difference results from differentiated accounting for agricultural land distribution between SMOKE and ISS methods and differentiated crop-nitrogen demands. Reduced fertilized area in ISS method results in reallocation of emissions in the ISS method. Positive values indicate a higher estimate of emissions in SMOKE method as compared to ISS method. The grid-level differences in emission estimates are summarized in Figure 4d. While a median difference of 0% is observed, the large error bar is indicative of the spatial differences in

emissions estimated by the ISS method compared to SMOKE. 58% of the grid cells exhibited more than $\pm 10\%$ difference in emissions between the two methods. Larger differences in emissions appear in grid cells located in regions with a larger heterogeneous mix of cropland or in grid cells where a smaller area of the grid is cropland with high nitrogen demand like a corn field. The ISS method is based on estimating contributions of emissions from crop-specific CFU. CFU for production of corn was the predominant contributor (95%) of NH_3 emissions in the Central Illinois domain, as expected due to the high nitrogen loading and widespread coverage of the crop in the domain in 2002.

3.2.2 Employing ISS Method to Quantify NH_3 Emissions for Midwest USA for Year 2011

The ISS method was employed to quantify NH_3 emissions at 4 km x 4 km resolution for a Midwest USA domain as shown in Figure 5a. Emission hotspots are observed to be dispersed across the domain and correspond to the presence of the Corn Belt in the States of Iowa to the west, Illinois in the center and Indiana in the eastern part of the domain. Additional hotspots are observed south of the domain and correspond to corn and cotton farms in the eastern part of Missouri. Figure 5b shows the percent differences in emissions calculated by SMOKE and the ISS method and is summarized in the box plot in Figure 5c. Differences in emissions between SMOKE and ISS methods, at the grid level, range from -423% to 99.7% , due to spatial reallocation of emissions by the ISS method. Difference in total NH_3 emissions estimated for the domain by SMOKE and ISS method is 1.75% , as these emissions are constrained by the same fertilizer sales data. However, differences in emissions between SMOKE and the ISS methods are greater than $\pm 15\%$ in 57% of the grid cells. The ISS method also provides the additional flexibility of identifying NH_3 emissions from CFU for specific crops. It is noteworthy that corn

cultivation in Midwest USA occupies 51% of the total agricultural land but contributes to 89% of NH₃ emissions from CFU. This is similar with trends reported for the smaller Central Illinois domain for 2002, where corn occupied 22% of the study domain and 55% of total agricultural land but contributed to 95% of emissions of NH₃ from CFU.

3.2.3 Comparison of the Proposed Emission Inventory with Existing Studies

NH₃ emission estimates used for the comparison between the ISS and SMOKE methods in this study are based on county-level fertilizer sales data for the year 2011. NEI for year 2011, however, reports NH₃ emissions from CFU using forecasted sales data, based on the rate of increase in sales between the years 2002 and 2007 [U.S. EPA, 2014]. Our approach indicates state level emission totals are within $\pm 3\%$ of NEI for all the states under consideration in the larger Midwest USA domain for year 2011. With regard to other NH₃ emission estimates from CFU, qualitative analysis of the observed spatial trends in emissions in the Midwest USA domain for 2011 using the ISS method showed consistency with the MASAGE model (spatial resolution 0.5° x 0.5°, years 2002-2005) [Paulot *et al.*, 2014]. Both methods identify emission hotspots over the Corn Belt in Iowa and Illinois. Estimates by MASAGE range between 910-1215 kg NH₃ km⁻² for Iowa and 604-911 kg km⁻² for Illinois. Our approach indicates emissions between 500-1233 kg NH₃ km⁻² for Iowa and 304-2376 kg NH₃ km⁻² for Illinois, partly due to the improved spatial heterogeneity represented by the ISS method. A quantitative comparison of emissions at county scale or grid scale was not possible with the MASAGE model due to differences in spatial resolution.

3.3 Temporal Variations in NH₃ Emissions from CFU in Test Study Domain using the DNDC Model

3.3.1 Daily Variability in NH₃ Emissions for 2002-2011

As previously mentioned, daily NH₃ emission factors were estimated using DNDC. The advantage of using DNDC is that it allows consideration of influences of crop management practices and weather and soil conditions, at local scales, as compared to SMOKE, where temporal factor estimates are based only on nitrogen use, as described in section 2.3.1.

Average DNDC-modeled NH₃ emissions and daily variability arising from the assumption of multiple dates of CFU at 13 sites, for the years 2002, 2005, 2008 and 2011, within the study domain are shown in Figure 6a. These years correspond to years when NEI is reported. Results are reported as percentage cumulative emissions for each Julian day averaged as the arithmetic mean over 13 sites. For each site, CFU input in terms of fertilizer type and amount was held constant for all years. Observed variations in emissions arise from variations in meteorological drivers of temperature, wind speed and rainfall and possible resulting changes in the soil environmental parameters during chosen CFU dates for the different crops, for the different years considered. Daily temporal factors averaged across these four years vary by $1.18\% \pm 1.52\%$. There is a marked difference in the timing and the strength of emission peaks. Emissions are first observed a month before planting of corn and soybeans between the third and last week of March. Large inter-annual variability (20%) is observed around the planting of corn and soybeans between the last week of April and first week of June. Emission peaks occur earlier in 2011 with 60% of cumulative emissions observed on day 100 as compared to days 110-125 for the other three years. Additional CFU a month after planting (day 150), results in an addition of 10% of the total emissions in 2011 and about 18% of total emissions in 2008. Remaining 20%

of the emissions are observed around the harvest of corn and soybeans and planting of winter wheat in late October to early November, in 2011.

In Figure 6b, we present cumulative percentage distribution of averaged NH_3 emissions and their associated variability as standard deviations based on DNDC modeling results spanning ten years and 13 sites as previously mentioned. Similar to Figure 6a, emissions are first observed a month prior to planting of corn and soybeans, in the second week of March, corresponding to nitrogen application in the spring before planting [USDA, 1997] and amount to 4% of the annual emissions. 78% of the total annual NH_3 emissions from CFU occur between the last week of March until early June, when planting and after-planting CFU occurs in the study domain. These peaks last between 2-8 days following individual events of CFU. The associated variability ranges from 2 to 10% on a daily scale across the 13 sites. This variability is particularly observed between days 97 and 120 and then between days of 142 and 165. Smaller emission peaks accounting for 18% of the total annual emissions are observed during fall, especially in mid-November. Overall, standard deviations in emissions estimated over 13 sites and 10 years is constrained within $\pm 10\%$ of the mean temporal estimate. This suggests that a single temporal factor profile could be used for different modeling years as input to air quality models, in the absence of year-specific data.

3.3.2 Comparison of the Proposed Temporal Factors with Existing Studies

Comparison of the average temporal factors (% NH_3 emitted per day) proposed in this study for the time period 2002-2011 using DNDC with the factors currently used in SMOKE are shown in Figure 7, for Midwest USA. Emission peaks identified by DNDC are unaccounted by the averaged temporal factors currently used in SMOKE. Ratio of temporal factors estimated on

a daily scale between SMOKE and DNDC methods is 0.54 ± 2.35 , indicating that on average, temporal factors used in SMOKE are about half the value of factors suggested by this study. This large standard deviation stems from the large emission peaks observed on some days in the year but low to zero emissions on other days within the same period. Emission peaks identified by this study occur 15 days or earlier compared to the temporal factors in SMOKE. Impacts related to NH_3 emissions such as $\text{PM}_{2.5}$ enhancement are typically episodic [Stanier *et al.*, 2012]; an understanding of underlying temporal trends in NH_3 emissions are invaluable for choosing time periods for CTM modeling studies to assess these impacts.

Figure 7 additionally includes temporal trends estimated by the semi-empirical, process-based approach used in the MASAGE model [Paulot *et al.*, 2014] and the inverse modeling approach [Gilliland *et al.*, 2006], on a monthly basis. Process-based approaches in the DNDC method and MASAGE model capture variability in NH_3 emissions, especially in months of CFU during planting (April-June) and post-harvest (October-November) in Midwest USA. Emission peaks are similarly identified in the months of April and May by the inverse modeling approach [Gilliland *et al.*, 2006], although magnitude and timing of emission peaks do not always coincide.

DNDC estimates, in this study, are consistent with reported measurement and modeling studies. A comprehensive review of these studies indicate that NH_3 volatilization occurs immediately after surface application of nitrogen, with 70-90% decrease observed in the first 24 hours [Sharpe and Harper, 1995] and that reduction in nitrogen volatilization continues a further 5-10 days after CFU [Sommer *et al.*, 2004]. NH_3 emissions were detected within four hours and decreased after 48 hours in a measurement study occurring after urea application [Rochette *et al.*,

2009]. *Ferrara et al.* [2014] identified nitrogen volatilization between 10-14% after urea applications, with reduced emissions ten days after urea application over a sorghum canopy.

3.4 Estimating Emission Factors for Three Commonly Used Fertilizers

Emission factors were estimated for urea, anhydrous ammonia and nitrogen solutions based on estimates from DNDC. For each fertilizer, DNDC runs were initiated separately for each crop type, for the 13 sites, by assuming state-specific crop nitrogen demands. The emission factors estimated in this study and the emission factors currently used in the NEI are shown in Table 3. The large standard deviation in modeled emissions suggests that a single value for emission factor does not sufficiently capture the uncertainty in volatilization patterns.

The mean NH₃ emission factor estimated by DNDC for urea is 17% lower than the value currently used in NEI. This mean emission factor falls within the observed in-situ measurements that range from 2.7% to 24% over a winter wheat canopy [*Ni et al.*, 2014], 19% to 20% for no-till and 4 to 5% for mold-board plowed soils [*Rochette et al.*, 2009]. Losses of nitrogen from urea have been reported in the range of 10% to 48% with a mean of 31% using micrometeorological methods in semi-arid conditions [*Sanz-Cobena et al.*, 2011]. For anhydrous ammonia, the mean emission factor modeled by DNDC is 0.7% as compared to the larger value used in NEI (1%), 30% smaller by difference. However, EEA reports a higher emission factor of 4% [EEA, 2002]. This indicates the need for better understanding of emission trends from anhydrous ammonia, which is a dominant form (34%) of nitrogen sales in USA [AAPFCO and The Fertilizer Institute, 2014].

Similarly, the mean emission factor for nitrogen solutions is 60% smaller than those currently used in NEI but exhibits large uncertainty. Emission factors currently used for nitrogen

solutions in NEI (8%) [Goebes *et al.*, 2003] are estimated by averaging the factors obtained for urea and ammonium nitrate from EEA. Our results (3.17%) are similar to emission factors measured (3.8%) over a corn canopy in Colorado, after application of nitrogen solutions [Jantalia *et al.*, 2012].

4.0 Conclusions

This study responds to the need to further develop emission inventories of precursor air pollutants, to support modeling efforts to improve predictions of regional particulate matter (PM) distribution and deposition of reactive nitrogen to ecosystems using chemical transport models. Our focus is on ammonia (NH₃) emissions from chemical fertilizer usage (CFU), which is the dominant source of NH₃ emissions in Midwest USA. Understanding of the spatial and temporal variability of NH₃ emissions from CFU at resolutions required by chemical transport models (CTMs) is currently limited by the sparse availability of in-situ measurements of NH₃ fluxes and absence of nitrogen management data at the farm level in USA. This study presents alternate approaches in developing an emission inventory at a high spatial resolution of 4 km x 4 km with a temporal resolution of a day by incorporating available knowledge of regional crop management practices, weather conditions and soil properties.

We developed the Improved Spatial Surrogate (ISS) method to allocate NH₃ emissions to areas receiving fertilizers at the higher spatial resolution of 4 km x 4 km by incorporating detailed spatial information on crop location and crop-specific nitrogen demands. For Midwest USA domain, for the year 2011, 57% of all grid cells estimated by ISS method indicated $\pm 15\%$ variability in NH₃ emissions from CFU as compared to spatial allocation of emissions in the Sparse Matrix Operator Kernel Emissions (SMOKE) model. The ISS method was tested for a

small domain and then an expanded domain. The method was applicable for Midwest U.S., given the available data sources, although some assumptions were needed to supply state-specific missing data. The ISS method can be used with different spatial resolutions and can thereby assist studies that aim to evaluate the influence of grid spacing of emissions inputs to predictions of PM formation and atmospheric deposition of sulfates and ammonium [Queen and Zhang, 2008; Appel *et al.*, 2011].

We also present an alternate approach to estimate daily temporal variations in NH₃ emissions from CFU by employing the process-based Denitrification Decomposition (DNDC) model. Our study is a significant contribution in view of the limited number of measurements of NH₃ emissions at time scales longer than a few days. Multi-year simulations indicate that daily variations in NH₃ emissions depend on soil conditions, fertilizer type and crop planting and harvesting dates. NH₃ emissions peak around the planting of corn and soybeans in Midwest USA. A smaller emission peak is observed in late fall, around the harvest of these crops and planting of winter wheat. DNDC thus provides a method to represent a higher resolution to the seasonality in emissions by identifying peaks occurring at daily scale based on local crop management and meteorological parameters. The study also demonstrates that the use of a single emission factor for urea, anhydrous ammonia and nitrogen solutions as used in the National Emissions Inventory may introduce uncertainties in estimating emissions as it does not account for influences of crop management practices and weather and soil conditions. The DNDC modeling approach resulted in lower emission factors for all fertilizers compared to the emission factors used in the National Emissions Inventory.

Efforts are being directed towards the validation of this proposed emissions inventory using measurements over a corn canopy for the entire growing season in Illinois. The spatially

and temporally resolved emissions inventory will also be combined with other precursor pollutants of concern to study the impact of CFU on regional PM concentrations and deposition of reactive nitrogen in Midwest USA.

Acknowledgments

This work is supported in part by NSF Award No AGS 12-36814 with an accompanying research experience for undergraduates (REU) and the University of Illinois Campus Research Board. Srinidhi Balasubramanian would like to acknowledge the Faculty for the Future Fellowship from the Schlumberger Foundation and the Ravindar K. and Kavita Kinra Fellowship from Civil and Environmental Engineering at the University of Illinois at Urbana-Champaign. The views reported here do not necessarily represent the views of these funding agencies. The authors thank Dr. Christopher Lehmann at the Illinois State Water Survey, National Atmospheric Deposition Program for support with data, Dr. Jia Deng at the University of New Hampshire for advice and support with DNDC and Meng Wang, undergraduate student supported by NSF-REU for assistance with preliminary DNDC modeling. The results for the developed emission inventory will be available upon request to the corresponding author (sotiriak@illinois.edu).

References

- AAPFCO and The Fertilizer Institute (2014), *Commercial Fertilizers*, Washington, DC.
- Available from: <http://www.aapfco.org/publications.html>. Last accessed December 2014.
- Aneja, V. P., J. Blunden, P. A. Roelle, W. H. Schlesinger, R. Knighton, D. Niyogi, W. Gilliam, G. Jennings, and C. S. Duke (2008), Workshop on agricultural air quality: State of the science, *Atmos. Environ.*, 42, 3195–3208, doi:10.1016/j.atmosenv.2007.07.043.

Appel, K. W., K. M. Foley, J. O. Bash, R. W. Pinder, R. L. Dennis, D. J. Allen, and K. Pickering (2011), A multi-resolution assessment of the Community Multiscale Air Quality (CMAQ) model v4.7 wet deposition estimates for 2002–2006, *Geosci. Model Dev.*, 4, 357–371, doi:10.5194/gmd-4-357-2011.

Asman, W. A. H. (1992), *Ammonia emissions in Europe: Updated emission and emission variations*, Report no. 228471008, National Institute of Public Health and Environmental Protection Bilthoven, Roskilde, Denmark.

Balasubramanian, S., M. Wang, S. Koloutsou-Vakakis, and M. J. Rood (2014), Modeling Temporal variability of gaseous ammonia emissions from chemical fertilizer usage in Midwest USA, in *107th Annual Conference & Exhibition, Air & Waste Management Association, Paper 33187*, pp. 1–17, Long Beach, California.

Bash, J. O., J. T. Walker, G. G. Katul, M. R. Jones, E. Nemitz, and W. P. Robarge (2010), Estimation of in-canopy ammonia sources and sinks in a fertilized Zea mays field, *Environ. Sci. Technol.*, 44(5), 1683–9, doi:10.1021/es9037269.

Bouwman, A. F., L. J. M. Boumans, and N. H. Batjes (2002), Estimation of global NH₃ volatilization loss from synthetic fertilizers and animal manure applied to arable lands and grasslands, *Global Biogeochem. Cycles*, 16(2), 8–1:8–11, doi:10.1029/2000GB001389.

CMAS (2013), SMOKE v3.5 User’s Manual. Available from: <https://www.cmascenter.org/smoke/>. Last accessed December 2014.

David, M. B., S. J. Del Grosso, X. Hu, E. P. Marshall, G. F. McIsaac, W. J. Parton, C. Tonitto, and M. A. Youssef (2009), Modeling denitrification in a tile-drained, corn and soybean agroecosystem of Illinois, USA, *Biogeochemistry*, 93, 7–30, doi:10.1007/s10533-008-9273-9.

EEA (2002), *Emission Inventory Guidebook: Agriculture -Third Edition*. Available from:
<http://www.eea.europa.eu/publications/EMEPCORINAIR3>. Last accessed September 2014.

EEA (2012), *Air quality in Europe - 2012 report*, Report no. 4/2012, Copenhagen, Denmark.

Erisman, J. W., A. Bleeker, J. Galloway, and M. S. Sutton (2007), Reduced nitrogen in ecology and the environment, *Environ. Pollut.*, 150, 140–149, doi:10.1016/j.envpol.2007.06.033.

Erisman, J. W., J. N. Galloway, S. Seitzinger, A. Bleeker, N. B. Dise, R. A. M. Petrescu, A. M. Leach, and W. de Vries (2013), Consequences of human modification of the global nitrogen cycle, *Philos. Trans. R. Soc. Ser. B.*, 368, doi:10.1098/rstb.2013.0116.

ESRI (2013), ArcGIS Desktop [computer software], Redland, California.

Farahbakhshazad, N., D. Dinnes, C. Li, D. Jaynes, and W. Salas (2008), Modeling biogeochemical impacts of alternative management practices for a row-crop field in Iowa, *Agric. Ecosyst. Environ.*, 123(1-3), 30–48, doi:10.1016/j.agee.2007.04.004.

Fernández, F. G., E. D. Nafziger, S. A. Ebelhar, and R. G. Hoeft (2012), Managing Nitrogen, in *Illinois Agronomy Handbook*, edited by E. D. Nafziger, pp. 113–132, University of Illinois.

Ferrara, R. M., B. Loubet, C. Decuq, A. D. Palumbo, P. Di Tommasi, V. Magliulo, S. Masson, E. Personne, P. Cellier, and G. Rana (2014), Ammonia volatilisation following urea fertilisation in an irrigated sorghum crop in Italy, *Agric. For. Meteorol.*, 195-196, 179–191, doi:10.1016/j.agrformet.2014.05.010.

Galloway, J. N., J. D. Aber, J. W. Erisman, S. P. Seitzinger, R. W. Howarth, E. B. Cowling, and B. J. Cosby (2003), The nitrogen cascade, *Bioscience*, 53(4), 341-356, doi:10.1641/0006-3568(2003)053[0341:TNC]2.0.CO;2.

Genermont, S., and P. Cellier (1997), A mechanistic model for estimating ammonia volatilization from slurry applied to bare soil, *Agric. For. Meteorol.*, 88, 145–167.

549 Gilliland, A. B., K. W. Appel, R. W. Pinder, and R. L. Dennis (2006), Seasonal NH₃ emissions
 550 for the continental United States: Inverse model estimation and evaluation, *Atmos.*
 551 *Environ.*, *40*, 4986–4998, doi:10.1016/j.atmosenv.2005.12.066.

552 Goebes, M. D., R. Strader, and C. Davidson (2003), An ammonia emission inventory for
 553 fertilizer application in the United States, *Atmos. Environ.*, *37*, 2539–2550,
 554 doi:10.1016/S1352-2310(03)00129-8.

555 Gopalakrishnan, G., M. Cristina Negri, W. Salas, and E. S. Division (2012), Modeling
 556 biogeochemical impacts of bioenergy buffers with perennial grasses for a row-crop field in
 557 Illinois, *GCB Bioenergy*, *4*(6), 739–750, doi:10.1111/j.1757-1707.2011.01145.x.

558 Gyldenkerne, S., C. A. Skj  th, O. Hertel, and T. Ellermann (2005), A dynamical ammonia
 559 emission parameterization for use in air pollution models, *J. Geophys. Res.*, *110*(D7),
 560 D07108, doi:10.1029/2004JD005459.

561 Heald, C. L., J. L. Collet Jr., T. Lee, K. B. Benedict, F. M. Schwandner, Y. Li, L. Clarisse, D. R.
 562 Hurtmans, M. Van Damme, C. Clerbaux, P.-F. Coheur, P.-F. S. Philip, R. V. Martin and
 563 H. O. T. Pye, (2012), Atmospheric ammonia and particulate inorganic nitrogen over the
 564 United States, *Atmos. Chem. Phys.*, *12*, 10295–10312, doi:10.5194/acp-12-10295-2012.

565 Henze, D. K., J. H. Seinfeld, and D. T. Shindell (2009), Inverse modeling and mapping US air
 566 quality influences of inorganic PM_{2.5} precursor emissions using the adjoint of GEOS-
 567 Chem, *Atmos. Chem. Phys.*, *9*, 5877–5903, doi:10.5194/acp-9-5877-2009.

568 Illinois State Water Survey (2014), Water and Atmospheric Resources Monitoring Program.
 569 Illinois Climate Network, Available from: <http://www.isws.illinois.edu/warm/datatype.asp>.
 570 Last accessed December 2014.

571 Jantalia, C. P., A. D. Halvorson, R. F. Follett, B. J. Rodrigues Alves, J. C. Polidoro, and S.
572 Urquiaga (2012), Nitrogen source effects on ammonia volatilization as measured with
573 semi-static chambers, *Agron. J.*, 104(6), 1595–1603, doi:10.2134/agronj2012.0210.

574 Li, C. (2000), Modeling trace gas emissions from agricultural ecosystems, *Nutr. Cycl.*
575 *Agroecosystems*, 58, 259–276, doi:10.1023/A:1009859006242

576 Li, C., S. Frolking, and T. A. Frolking (1992), A model of NO evolution from soil driven by
577 rainfall events 1. Model structure and sensitivity, *J. Geophys. Res.*, 97(D9), 9759–9776,
578 doi:10.1029/92JD00509

579 Microsoft (2013), Microsoft Access [computer software], Redmond, Washington.

580 Myles, L., J. Kochendorfer, M. W. Heuer, and T. P. Meyers (2011), Measurement of trace gas
581 fluxes over an unfertilized agricultural field using the flux-gradient technique, *J. Environ.*
582 *Qual.*, 40, 1359–1365, doi:10.2134/jeq2009.0386.

583 Myles, L., S. Koloutsou-Vakakis, C. M. B. Lehmann, R. D. Saylor, M. Heuer, D. Sibble, J.
584 Caldwell, S. Balasubramanian, A. Nelson, and M. J. Rood (2014), NH₃ emission from
585 fertilizer application: A collaborative study in the Midwestern U.S, in *2014 AGU Fall*
586 *Meeting*, San Francisco, California.

587 NADP (2014), National Trends Network, *National Atmospheric Deposition* Program. Available
588 from: <http://nadp.sws.uiuc.edu/NTN/ntnData.aspx>. Last accessed September 2014.

589 NASS (2003), *Agricultural Chemical Usage 2002 Field Crops Summary, Ag Ch 1 (03)*, US
590 Department of Agriculture, Washington DC.

591 NASS (2010), *Field Crops Usual Planting and Harvesting Dates, Agricultural Handbook*
592 *Number 628*, US Department of Agriculture.

593 NASS (2014a), *2012 Census of Agriculture: United States Summary and State Data*, Volume 1,
594 US Department of Agriculture.

595 NASS (2014b), *Census of Agriculture Database*, *US Department of Agriculture*. Available from:
596 <http://quickstats.nass.usda.gov/>. Last accessed November 2014.

597 NASS (2014c), *Crop. Data Layer*, *US Department of Agriculture*. Available from:
598 <http://nassgeodata.gmu.edu/CropScape/>. Last accessed November 2014.

599 Nelson, A. J., M. Vieira-Filho, C. M. B. Lehmann, L. Myles, S. Koloutsou-Vakakis, and M. J.
600 Rood (2014), Measurement of Bi-Directional Ammonia Exchange Above a Mize Canopy
601 in the Midwestern United States, in *2014 AGU Fall Meeting*, San Francisco, California.

602 Ni, K., A. Pacholski, and H. Kage (2014), Ammonia volatilization after application of urea to
603 winter wheat over 3 years affected by novel urease and nitrification inhibitors, *Agric.*
604 *Ecosyst. Environ.*, *197*, 184–194, doi:10.1016/j.agee.2014.08.007.

605 NRCS (2013), *Web Soil Survey*, *USDA Natural Resources Conservation Service*. Available
606 from: <http://websoilsurvey.nrcs.usda.gov/>. Last accessed November 2014.

607 Pardo, L. H., M. E. Fenn, C. L. Goodale, L. H. Geiser, C. T. Driscoll, E. B. Allen, J. S. Baron, R.
608 Bobbink, W. D. Bowman, C. M. Clark, B. Emmett, F. S. Gilliam, T. L. Greaver, S. J. Hall,
609 E. A. Lilleskov, L. Liu, J. A. Lynch, K. J. Nadelhoffer, S. S. Perakis, M. J. Robin-Abbot, J.
610 L. Stoddard, K. C. Weathers and R. L. Dennis (2011), Effects of nitrogen deposition and
611 empirical nitrogen critical loads for ecoregions of the United States, *Ecol. Appl.*, *21*(8),
612 3049–3082, doi:10.1890/10-2341.1

613 Paulot, F., D. J. Jacob, R. W. Pinder, J. O. Bash, K. Travis, and D. K. Henze (2014), Ammonia
614 emissions in the United States, European Union, and China derived by high-resolution
615 inversion of ammonium wet deposition data : Interpretation with a new agricultural

emissions inventory (MASAGE_NH3), *J. Geophys. Res. Atmos.*, 119, 4343–4364,
doi:10.1002/2013JD021130.

Phillips, S., S. Pal Arya, V. P. Aneja (2004), Ammonia flux and dry deposition velocity from
near-surface concentration gradient measurements over a grass surface in North Carolina,
Atmos. Environ., 38, 3469–3480, doi:10.1016/j.atmosenv.2004.02.054.

Pinder, R. W., P. J. Adams, and S. N. Pandis (2007), Ammonia emission controls as a cost-
effective strategy for reducing atmospheric particulate matter in the eastern United States,
Environ. Sci. Technol., 41(2), 380–386, doi:10.1021/es060379a.

Pinder, R. W., A. B. Gilliland, and R. L. Dennis (2008), Environmental impact of atmospheric
NH3 emissions under present and future conditions in the eastern United States, *Geophys.*
Res. Lett., 35(12), 1–6, doi:10.1029/2008GL033732.

Pinder, R. W., J. T. Walker, J. O. Bash, K. E. Cady-Pereira, D. K. Henze, M. Luo, G. B.
Osterman, and M. W. Shephard (2011), Quantifying spatial and seasonal variability in
atmospheric ammonia with in situ and space-based observations, *Geophys. Res. Lett.*, 38,
1–5, doi:10.1029/2010GL046146.

Potter, C., C. Krauter, and S. Klooster (2001), *Statewide Inventory Estimates of Ammonia*
Emissions from Native Soils and Chemical Fertilizers in California, ARB Contract Number
ID 98-716, California State University, Fresno, California.

Pouliot, G., T. Pierce, H. Denier van der Gon, M. Schaap, M. Moran, and U. Nopmongkol
(2012), Comparing emission inventories and model-ready emission datasets between
Europe and North America for the AQMEII project, *Atmos. Environ.*, 53, 4–14,
doi:10.1016/j.atmosenv.2011.12.041.

638 Queen, A., and Y. Zhang (2008), Examining the sensitivity of MM5–CMAQ predictions to
 639 explicit microphysics schemes and horizontal grid resolutions, Part III—The impact of
 640 horizontal grid resolution, *Atmos. Environ.*, *42*, 3869–3881,
 641 doi:10.1016/j.atmosenv.2008.02.035.

642 Rochette, P., D. A. Angers, M. H. Chantigny, J. D. MacDonald, N. Bissonnette, and N. Bertrand
 643 (2009), Ammonia volatilization following surface application of urea to tilled and no-till
 644 soils: A laboratory comparison, *Soil Tillage Res.*, *103*, 310–315,
 645 doi:10.1016/j.still.2008.10.028.

646 Sanz-Cobena, A., T. Misselbrook, V. Camp, and A. Vallejo (2011), Effect of water addition and
 647 the urease inhibitor NBPT on the abatement of ammonia emission from surface applied
 648 urea, *Atmos. Environ.*, *45*, 1517–1524, doi:10.1016/j.atmosenv.2010.12.051.

649 Saylor, R. D., L. Myles, D. Sibble, J. Caldwell, and J. Xing (2014), Recent trends in gas-phase
 650 ammonia and PM_{2.5} ammonium in the southeast United States, *J. Air Waste Manage.*
 651 *Assoc.*, 1-34, doi:10.1080/10962247.2014.992554.

652 Sharpe, R. R., and L. A. Harper (1995), Soil, plant and atmospheric conditions as they relate to
 653 ammonia volatilization, *Fertil. Res.*, *42*, 149–158, doi:10.1007/BF00750509.

654 Simmons, F. W., and E. D. Nafziger (2012), Soil Management and Tillage, in *Illinois Agronomy*
 655 *Handbook*, edited by E. D. Nafziger, pp. 133–142, University of Illinois.

656 Skjøth, C. A., C. Geels, H. Berge, S. Gyldenkerne, H. Fagerli, T. Ellermann, L. M. Frohn, J.
 657 Christensen, K. M. Hansen, K. Hansen and O. Hertel (2011), Spatial and temporal
 658 variations in ammonia emissions – a freely accessible model code for Europe, *Atmos.*
 659 *Chem. Phys.*, *11*, 5221–5236, doi:10.5194/acp-11-5221-2011.

660 Sommer, S. G., J. K. Schjoerring, and O. T. Denmead (2004), Ammonia emission from mineral
 661 fertilizers and fertilized crops, *Adv. Agron.*, 82, doi:10.1016/S0065-2113(03)82008-4.
 662 Stanier, C., A. Singh, W. Adamski, J. Baek, M. Caughey, G. R. Carmichael, E. Edgerton, D.
 663 Kenski, M. Koerber, J. Oleson, T. Rohlf, S. R. Lee, N. Reimer, S. Shaw, S. Sousan and S.
 664 N. Spak, (2012), Overview of the LADCO winter nitrate study: hourly ammonia, nitric acid
 665 and PM_{2.5} composition at an urban and rural site pair during PM_{2.5} episodes in the US
 666 Great Lakes region, *Atmos. Chem. Phys.*, 12, 11037–11056, doi:10.5194/acp-12-11037-
 667 2012.
 668 Tonitto, C., M. B. David, L. E. Drinkwater, and C. Li (2007), Application of the DNDC model to
 669 tile-drained Illinois agroecosystems: model calibration, validation, and uncertainty
 670 analysis, *Nutr. Cycl. Agroecosystems*, 78, 51–63, doi:10.1007/s10705-006-9076-0.
 671 U.S. Census Bureau (2011), TIGER/Line® Shapefiles, Available from:
 672 <https://www.census.gov/geo/maps-data/data/tiger-line.html>. Last accessed May 2014.
 673 U.S. EPA (2002), Temporal Allocation of Annual Emissions Using EMCH Temporal Profiles
 674 Date, *Memo. EPA*.
 675 U.S. EPA (2003), Projected Costs, *2003 Tech. Support Packag. Clear Ski*. Available from:
 676 http://www.epa.gov/air/clearskies/03technical_package_sectionc.pdf. Last accessed May
 677 2014.
 678 U.S. EPA (2005), Spatial Surrogate Documentation, Available from:
 679 http://www.epa.gov/ttn/chief/emch/spatial/new/surrogate_documentation_workbook06300
 680 5.xls. Last accessed November 2014.

681 U.S. EPA (2011), Reactive Nitrogen in the United States: An Analysis of Inputs, Flows,
682 Consequences, and Management Options. Available from: <http://www.epa.gov/sab>. Last
683 accessed January 2015.

684 U.S. EPA (2012), National Ambient Air Quality Standards, Available from:
685 <http://www.epa.gov/air/criteria.html>. Last accessed January 2015.

686 U.S. EPA (2013), National Emissions Inventory Data & Documentation, Available from:
687 <http://www.epa.gov/ttnchie1/net/2002inventory.html>. Last accessed March 2014.

688 USDA (1997), *Agricultural Resources and Environmental Indicators, 1996-97. Agricultural*
689 *Handbook No. 712*, USDA, Economic Research Service, Washington DC.

690 Vogelmann, J. E., S. M. Howard, L. Yang, C. R. Larson, B. K. Wylie, and N. Van Driel (2001),
691 Completion of the 1990s National Land Cover Data set for the conterminous United States
692 from Landsat Thematic Mapper data and ancillary data sources, *Photogramm. Eng. Remote*
693 *Sens.*, 67, 650–662.

694 Walker, J., W. Robarge, Y. Wu, and T. Meyers (2006), Measurement of bi-directional ammonia
695 fluxes over soybean using the modified Bowen-ratio technique, *Agric. For. Meteorol.*,
696 138(1-4), 54–68, doi:10.1016/j.agrformet.2006.03.011.

697 Walker, J. T., M. R. Jones, J. O. Bash, L. Myles, T. Meyers, D. Schwede, J. Herrick, E. Nemitz,
698 and W. Robarge (2013), Processes of ammonia air–surface exchange in a fertilized Zea
699 mays canopy, *Biogeosciences*, 10, 981–998, doi:10.5194/bg-10-981-2013.

700 WHO (2005), *Air quality guidelines for particulate matter, ozone, nitrogen dioxide and sulfur*
701 *dioxide*. Available from
702 http://www.who.int/phe/health_topics/outdoorair/outdoorair_aqg/en/. Last accessed
703 November 2014.

704 Wu, S.-Y, S. Krishnan, Y. Zhang, and V. Aneja (2008), Modeling atmospheric transport and fate
 705 of ammonia in North Carolina—Part I: Evaluation of meteorological and chemical
 706 predictions, *Atmos. Environ.*, *42*, 3419–3436, doi:10.1016/j.atmosenv.2007.04.031.
 707 Xu-Ri, M. Wang, and Y. Wang (2003), Using a modified DNDC model to estimate N₂O fluxes
 708 from semi-arid grassland in China, *Soil Biol. Biochem.*, *35*, 615–620, doi:10.1016/S0038-
 709 0717(03)00009-9.
 710 Zhu, L., D. K. Henze, K. E. Cady-Pereira, M. W. Shephard, M. Luo, R. W. Pinder, J. O. Bash,
 711 and G.-R. Jeong (2013), Constraining U.S. ammonia emissions using TES remote sensing
 712 observations and the GEOS-Chem adjoint model, *J. Geophys. Res. Atmos.*, *118*(8), 3355–
 713 3368, doi:10.1002/jgrd.50166.

714 **Table 1.** Comparison of spatial surrogates for estimating NH₃ emissions from chemical fertilizer usage in SMOKE and ISS methods
715 for year 2002

Method	Surrogate	Resolution	Spatial Attributes	Spatial Surrogate Ratio (SSR)
SMOKE	NLCD for year 1992	1 km x 1 km	5 agricultural categories including row crops, small grains, pasture/hay, fallow and urban grasses	$SSR_z = \frac{\sum_j A_{j,z}}{\left(\sum_z \sum_j A_{j,z} \right)_q}$
ISS	CDL for year 2002	30 m x 30 m	108 crops (e.g.: corn) including double cropped varieties (e.g.: double cropped corn and soybeans)	$SSR_z = \left(\frac{\sum_j R_j A_{j,z}}{\sum_z \sum_j R_j A_{j,z}} \right)_q$

$A_{j,z}$: Area of crop 'j' (km²) in grid cell 'z' located in county 'q'

R_j : kg-N applied per unit area for crop 'j'

716

717 **Table 2.** An example of the data and calculations used in estimating timing and amount of nitrogen applied to corn in the state of
718 Illinois

Crop area ^a		Area receiving nitrogen (%) ^b				Nitrogen loading (kg/acre) ^c				Seasonal contribution of nitrogen loading (%) ^d				Planting and harvesting dates ^e		Chosen planting and harvesting dates ^f	
Nitrogen treated crop area (%)	Planted area (km ²)	FBP _g	AP _g	AFP _g	SBP _g	FBP	AP	AFP	SBP	FBP	AP	AFP	SBP	PD _g	HD _g	PD	HD
98	50,990	46	7	23	75	33	9	48	45	25.7	1	18.3	55	Apr 21 – May 23	Sept 23 – Nov 20	Apr 21, May 1, May 14, May 23	Oct 23, Nov 20

719 ^a Data obtained from NASS [2003]

720 ^b Percentage area receiving nitrogen in four different crop periods. Total is $\geq 100\%$ due to multiple applications [USDA, 1997]

721 ^c Nitrogen loading in different crop period (kg/acre) [USDA, 1997]. 1 acre corresponds to 0.004047 km²

722 ^d Calculated as the percentage of nitrogen loading in each crop period compared to the annual nitrogen loading of the particular crop
723 type.

724 Nitrogen loading in crop period = planted area^a x nitrogen treated area^a x % area receiving nitrogen in the crop period^b x nitrogen
725 loading in the crop period^c

726 ^e Typical planting and harvesting dates are based on CFU dates reported over a 20 year period [NASS, 2010]

727 ^f Chosen planting and harvesting dates in this study as explained in Section 2.3.2.2

728 ^g Crop periods: FBP = Fall before planting, AP = at planting, AFP = after planting, SBP = spring before planting, PD = planting date,
729 HD = harvesting date

730 **Table 3.** Comparison of emission factors for urea, anhydrous ammonia and nitrogen solutions
 731 estimated in this study using DNDC with the values used in the National Emissions Inventory

Fertilizer	Emission factors (%) estimated in this study	Emission factors (%) used in NEI [<i>Goebes et al.</i>, 2003]
Urea	14.2 ± 8.6	18
Anhydrous Ammonia	0.7 ± 1.76	1
Nitrogen Solutions	3.17 ± 4.37	8

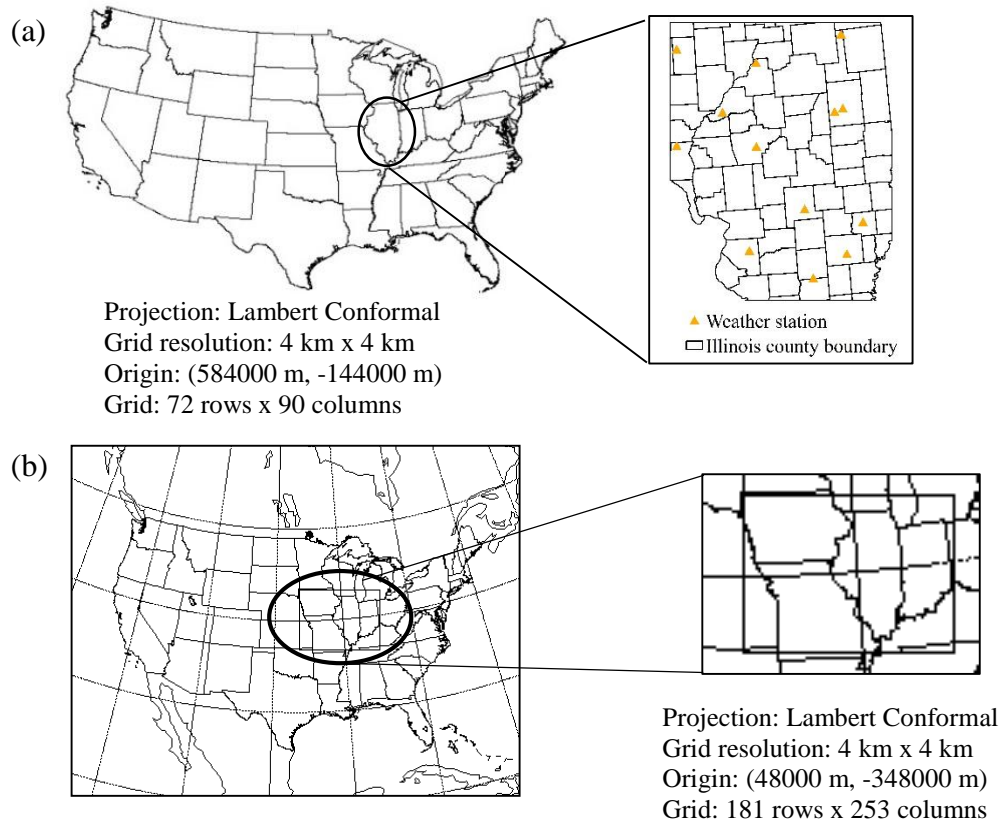


Figure 1. (a) Location of the test domain relative to contiguous USA and the state of Illinois chosen to demonstrate the ISS method. Also shown 13 weather stations of interest (b) Extended Midwest USA study domain. The location of the domain is indicated relative to contiguous USA. Grid parameters are listed for both the test domain and expanded domain.

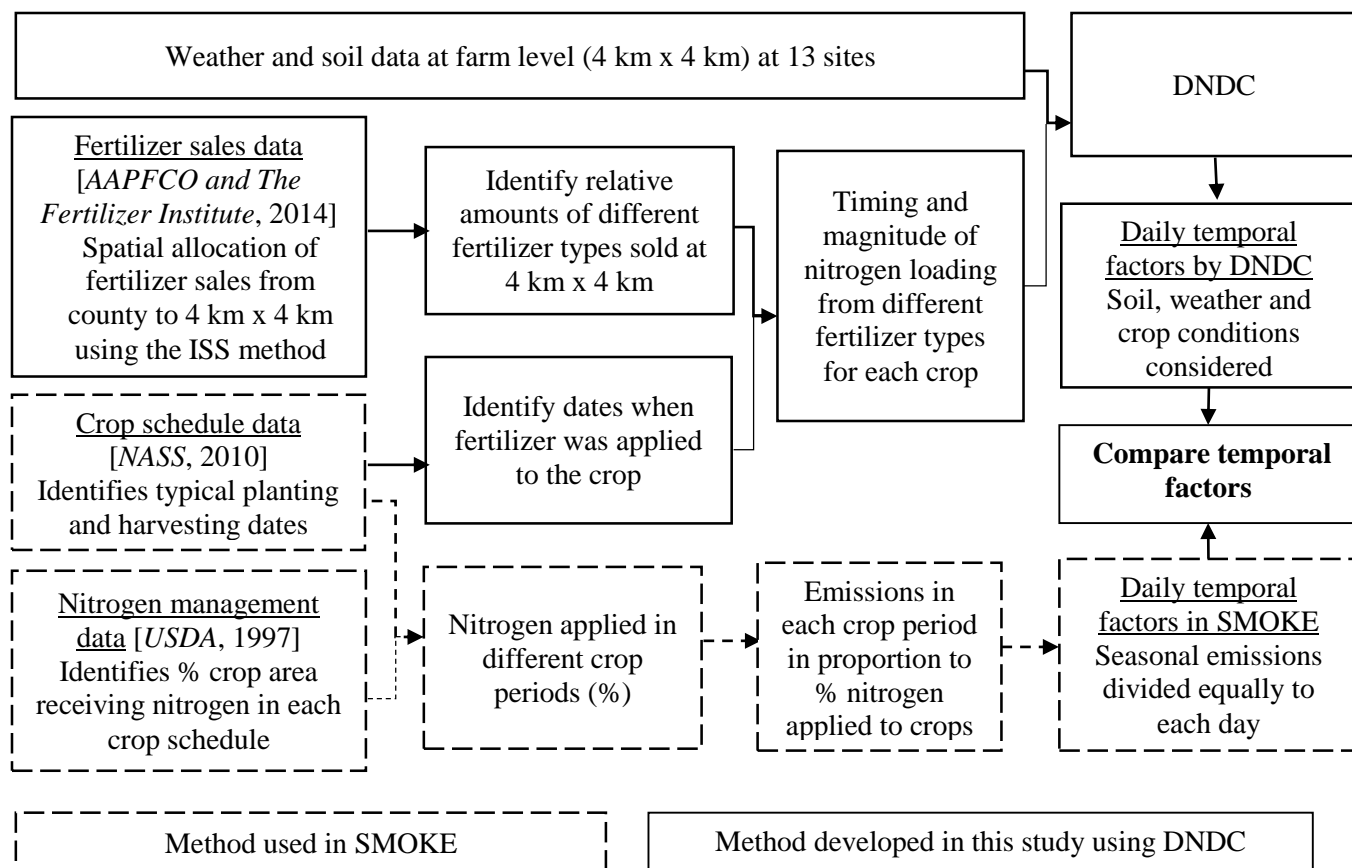


Figure 2. Modeling scheme adopted in this study to estimate temporal factors using DNDC.

Comparisons of the existing approach in SMOKE and the contributions from this study are indicated.

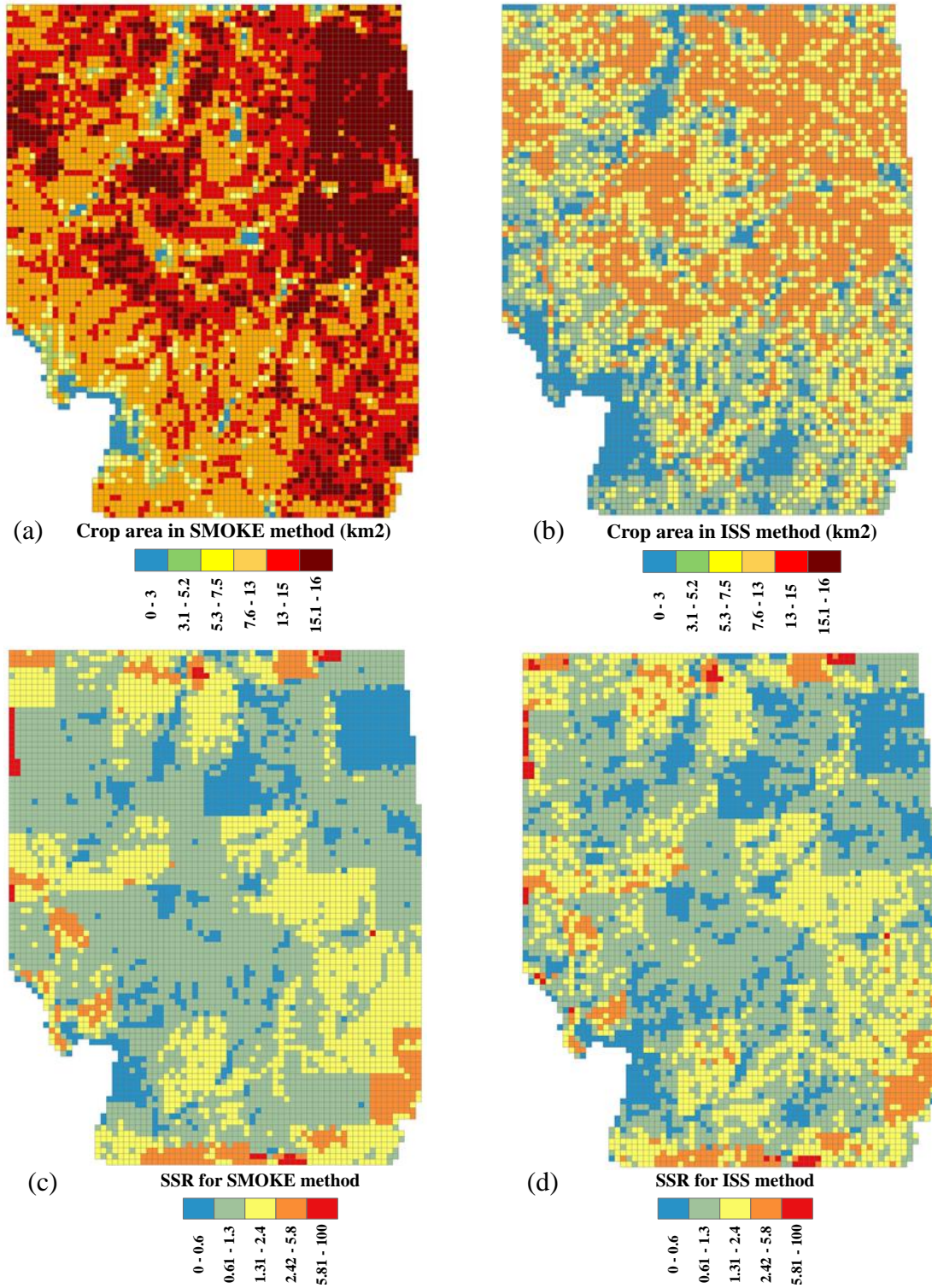


Figure 3. The top figures indicate the allocation of crop land (km²) receiving chemical fertilizers in the test domain over Central Illinois in the (a) SMOKE method and (b) ISS method. The

741 bottom figures represent the SSRs calculated for NH₃ emissions from CFU (c) in SMOKE
742 method and (d) the ISS method.

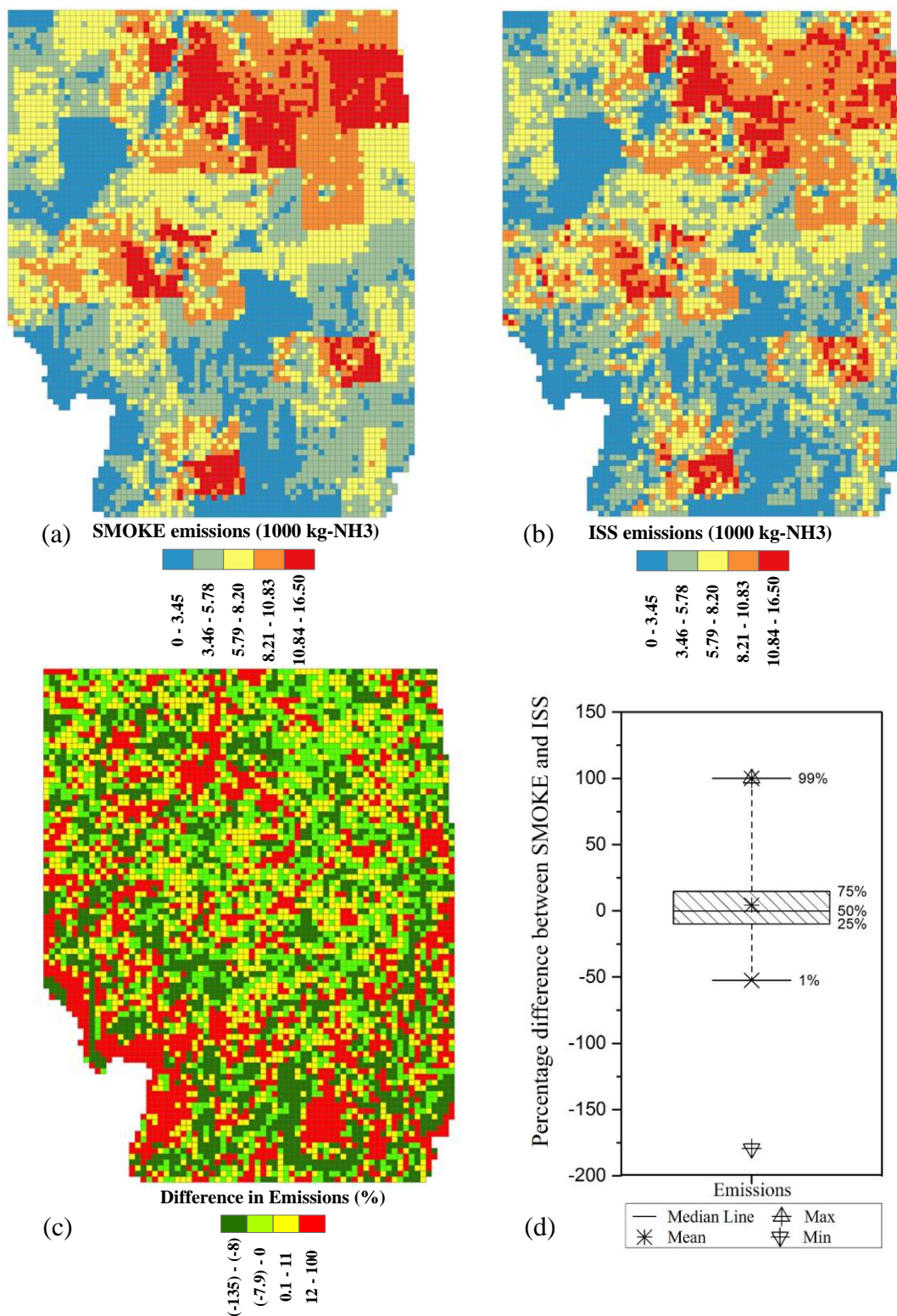
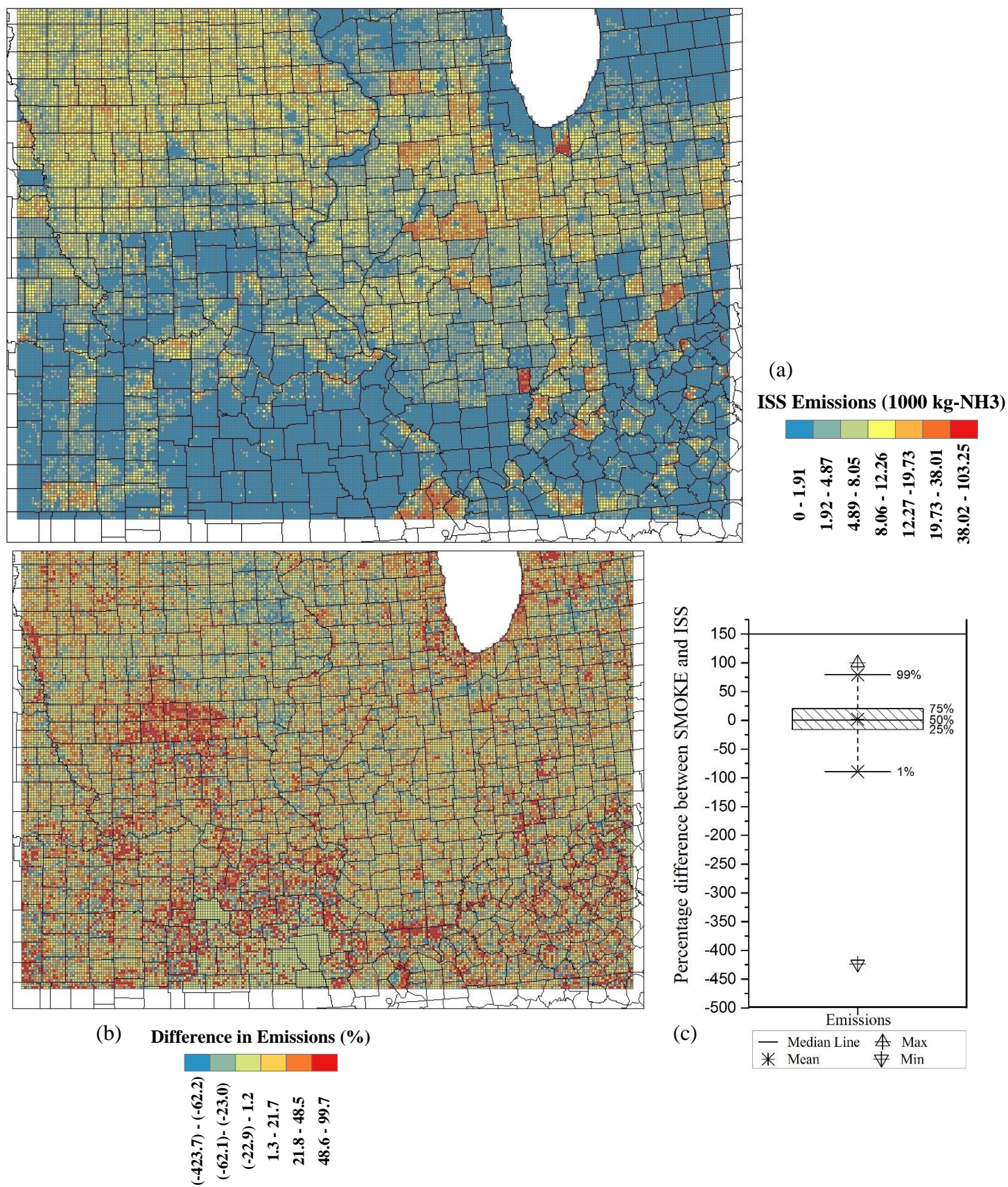


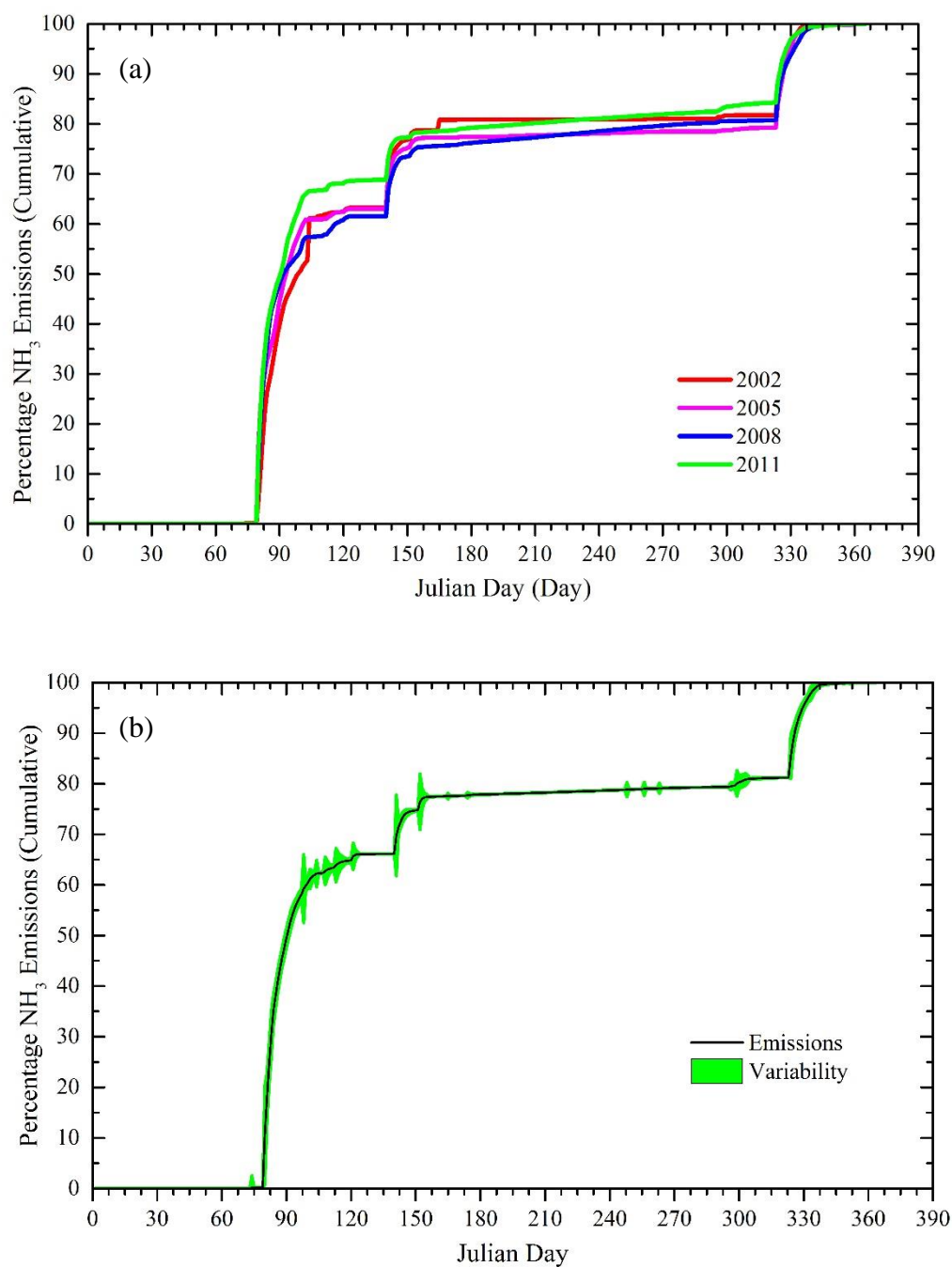
Figure 4. The top figures represent NH₃ emissions (1000 kg-NH₃ yr⁻¹) emitted from CFU from each 4 km x 4 km grid cell for the test domain over Central Illinois as estimated (a) in SMOKE

745 and (b) ISS method. The bottom figures represent the percentage differences in NH_3 emissions
746 from CFU between SMOKE and ISS methods represented at (c) the grid level and (d)
747 summarized as a box plot. The box plot represents the distribution percent difference in NH_3
748 emissions from CFU between SMOKE and ISS methods where positive values indicates grids
749 where emissions measured by SMOKE method was greater than ISS method.



750 **Figure 5.** (a) NH₃ emissions (1000 kg-NH₃ yr⁻¹) from CFU estimated using ISS method for the

751 year 2011 for the extended Midwest USA domain. The bottom figures represent the percentage
752 differences in NH_3 emissions from CFU between SMOKE and ISS methods represented at the
753 (B) grid level and (C) summarized as a box plot. The box plot represents the distribution percent
754 difference in NH_3 emissions from CFU between SMOKE and ISS methods where positive values
755 indicates grids where emissions measured by SMOKE method was greater than ISS method.



756 **Figure 6:** Variations in NH_3 emissions averaged over 13 sites. (a) Compares the mean temporal
 757 factor profile for the years reported in NEI (2002, 2005, 2008, 2011) (b) Temporal factors for
 758 NH_3 emissions from CFU averaged over 13 sites and 10 years. Variability is reported at the daily
 759 scale as the standard deviation of 1320 model runs.

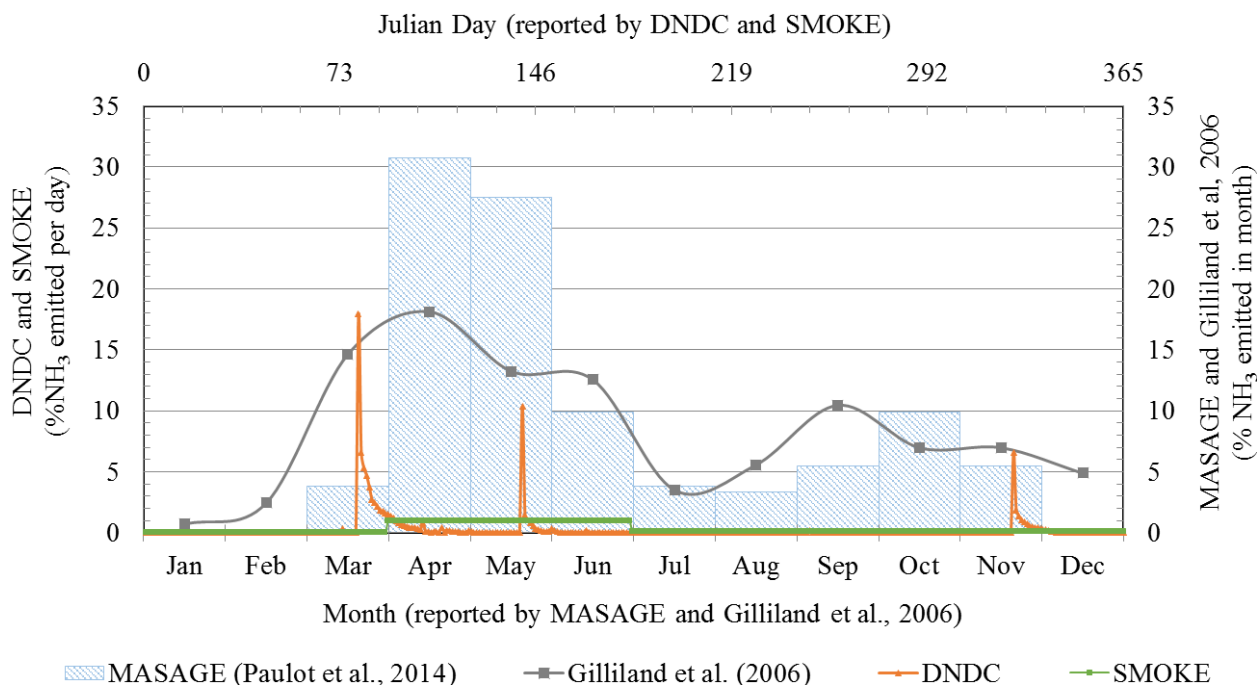


Figure 7. Comparison of temporal factors for NH₃ emissions from CFU proposed by this study (DNDC) with literature values. Temporal factors are defined as percentage NH₃ emitted in a particular time span. Temporal factors are reported at daily scale for DNDC and SMOKE methods and at the monthly scale for the MASAGE model and Gilliland et al. (2006).